Proceedings of the 1999 IEEE/ASME
International Conference on Advanced Intelligent Mechatronics
September 19-23, 1999 • Atlanta, USA

Modeling of the Natural Product Deboning Process Using Biological and Human Models

Wayne Daley[+], Tian He*, Kok-Meng Lee*, Melissa Sandlin**
[+]Georgia Tech Research Institute, Georgia Institute of Technology, Atlanta, GA 30332-0823
**School of Mechanical Engineering, Georgia Institute of Technology, Atlanta, GA 30332-0405*

Abstract--One critical area in automation for commercial deboning systems for meat processing, is the inability of existing equipment to adapt to varying sizes and shapes of products. This usually results in less than desirable outcomes when measured in terms of yield of the operations. In poultry processing for example, the initial cut of wing-shoulder joints is the most critical step in the deboning process. Two approaches for determining a trajectory for the cut is presented. The first is a technique using x-ray and visual images to obtain a 2-D model that locates the shoulder joint with respect to the surface features of the product. The second approach is obtained by determining a 3-D cutting trajectory and the associated forces/torques using a motion analysis system and a force/torque sensor incorporated with a knife. We then discuss the potential application of these results in the design of an automated cutting system that uses the obtained trajectory as a nominal cutting path. The system would make adjustments during the cut using force feedback so as to emulate the manual cutting process.

Index terms--deboning, natural product cutting, automation, machine vision, motion tracking, human performance emulation

I. INTRODUCTION

There has been a drastic increase in the demand for preprocessed (sectioned, deboned) natural products like meat, fish, and poultry. As shown in Figure 1 (dark portion), over a period of 16 years, there was a very large increase in the amount of broiler exports of deboned and further processed products [1].

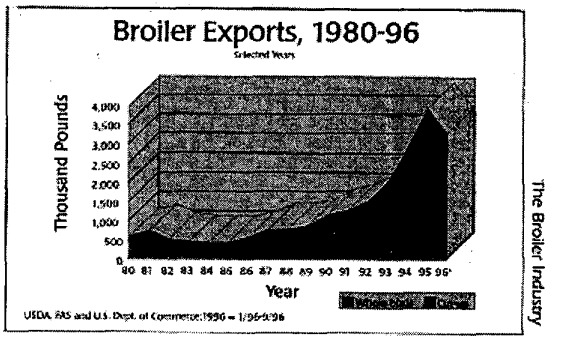

Figure 1. Broiler exports trend, 1980-1996

Deboning is a job that requires a lot of dexterity, which is usually performed manually in food industries. The repetitive motions made up to many thousands of times per day make poultry-processing workers suffer much more disorders of the hand, wrist, and shoulder than workers in other industries [2]. This, in addition to the increase in demand for further processed products, along with the decreasing availability of labor provides a major incentive for the poultry industry to automate many processing and deboning operations of their further process.

There are several automated poultry deboning systems available in the market. The Johnson-Baader Breast Deboner [3] uses a set of knives and skinners to perform the deboning in 15 steps. FoodCraft's Poultry Modular Breast Deboning System [4] utilizes an initial cut with mechanical separation. Mycom's Toridas Automated Poultry Leg Deboning Robot [5] uses an 8-step manipulation with a few measurements to accomplish poultry leg deboning. All the other approaches involve little or no ability for dynamic compensation for varying sizes and shapes of products, thus currently do not achieve desired yields.

Khodabandehloo [6] and Purnell [7] reported the development of a vision guided, knowledge based robotic meat cutting system with a force feedback mechanism for the forequarter beef cutting. The 3 dimensional profile of the carcass obtained by two CCD cameras is compared with the predetermined models of carcasses stored in a database and used to generate an initial cutting path. A multi-DOF robot arm performs the cut following the path while making adjustments according to the force feedback. Lay [8] developed a similar pork loin deboning system with force feedback control implemented using fuzzy logic. It should be noted that the rigidity and ease of fixturing for beef and pork products are not available for poultry products.

Silva and Wickramarachchi [9] developed a vision based integrated system for head cutting of fish. The fish image captured by a CCD camera is processed to detect fish features, which are used to accurately position the cutter with respect to the fish. Increases of 2.1% to 4.4% have been achieved in the end product weight. The vision guided positioning applied in the system is basically a 1 dimensional procedure, which limits the system to the specific fish head removal application and reduces its potential for other natural product cutting tasks. Malone et. al. [10] constructed a vision based cutting system with knowledge based control for removal of the lateral pin bones from fish fillets. Images of fish fillets obtained by a CCD camera are processed to locate the bone area and then used to generate the cutting path, which is followed by a high pressure waterjet. Insufficient contrast between the bone and meat coupled with the lack of accurate quantitative information from prior knowledge led to pretty poor system performance. A similar system was also reported by Jacobs [11]. These systems could only handle 2 dimensional, planar cutting procedures, making them incapable in more general cutting tasks that usually require 3 dimensional manipulation of the cutting tool.

Some similarities can be found between automated deboning and robotics in surgery. Most of the surgical robots involve the acquisition and representation of 3D model using images from CCD cameras or other devices like magnetic resonance, CT, laser, and x-ray [12][13]. The recognition of significant features and accurate quantitative measurement are often required. The ideal cutting path for automated deboning process directly depends on the relationship between the internal bone structure and the external features, which also happens in computer assisted surgery [14]. The similarities in the two areas make the experience in the surgical robot useful for the automatic deboning process and provide some basis for the biological model to be described below.

II. OVERVIEW

The focus of this research is in the area of further processing; in particular, front half deboning. Once a product reaches the further processing stage, it is without hindquarters, head and neck, and consists of the upper half with the wings. An example of a processing line can be seen in Figure 2.

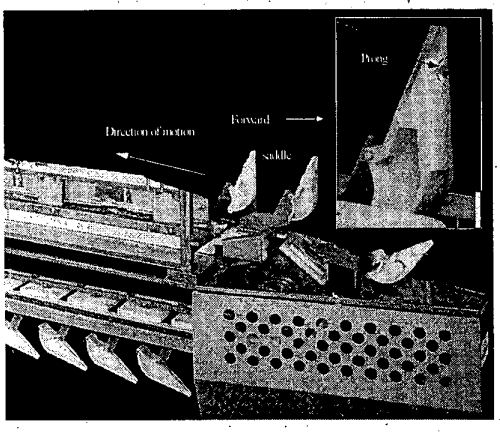

Figure 2. Saddle and example processing line

An employee places the upper half onto one saddle, which is connected to a moving processing line. The force of gravity acting on the product holds it onto the saddle and a prong on the front of the saddle restrains the product from rotating. The main purpose of the saddle is to orient, locate, and fixture the product.

The metric for optimization in the deboning process is percent yield. This is the weight of the boneless meat (the end product) over that of the pre-processed product weight. Another technique such as "scrape" is used where you look at the amount of meat left on some key areas of the carcass. In one poultry processing plant using a system in which on-line workers perform the initial cut and subsequent steps are automated. The average percent yield for the semi-automated process is 45.4% over a period of one year and one month. The range for this time period was 41.7 – 47.2%. In the current system, the skill of the workers has a significant impact on the variation in percent yield. Other factors such as fatigue, boredom, or injury also contribute to a lower yield. An automated system, on the other hand, has another set of factors that need to be considered. These include size and orientation variation, time to process, and contamination. In the automated system, any variation in size and orientation will have to be compensated for. In addition, contamination must be minimized or eliminated. The time it takes to process must be comparable to that of human workers.

It has been empirically observed that the initial cut is the main contributing factor to the percent yield. A cut that is too close will nick bone and contaminate the product. On the other hand, if a conservative cut is made, the percent yield will be sub-optimal.

There are two aspects to be considered; these are first, knowing where to cut (i.e. what is the cutting path) and second, actually executing the cut. This paper is concerned with the first task and the approaches that could be used to determine workable cutting trajectories.

In this paper we will examine two approaches for generating models for accomplishing cutting tasks of variable and flexible products. The first relies on the use of biological models of the products while the second utilizes empirical data acquired from people actually doing the task. We look at the biological models in section III. The human-generated model will be examined in section IV. We then conclude with a description of future work in section V.

III. BIOLOGICAL MODEL GENERATION

In deboning the cutting operations are directly dependent on the internal structure relative to the surface features of the object of interest. Therefore, it is desired that before an initial cut is performed, some knowledge of the internal structure be deduced from the external features. The bones involved in this process are illustrated in Figure 3. The initial cut starts at the front part of the neck opening, continues around the shoulder knuckle of the humerus, severing the tendons in the joint, and follows through the back side along the scapula. Figure 4 (a) shows a chicken sample before the initial cut, while Figure 4 (b) shows the dismembered joint after the tendons supporting the joint are severed. This is a good cut illustrated by the clean separation of the ball and the socket.

A. Experimental setup

We develop, in this section, a biological model using a combination of an x-ray image to obtain the internal bone structure and a visual image to obtain surface features of the same object. We then use these two images to construct a model that correlates between external features and internal bird structure.

The experimental setup, has three main components; namely, the digital external imaging system, the x-ray imaging system and the calibration board, is shown in Figure 5. The bird sample is put on the saddle. The x-ray source emits x-rays in a conical

beam, while the detector camera behind an image intensifier (not shown in the figure) captures the x-ray image. The calibration board, which is fixed with respect to the saddle, is used as a common reference frame for both the external imaging and the x-ray imaging systems.

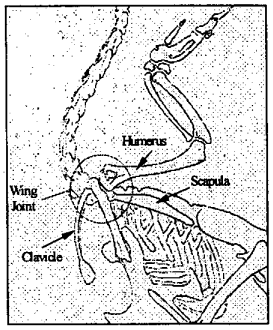

Figure 3. Chicken anatomical structure

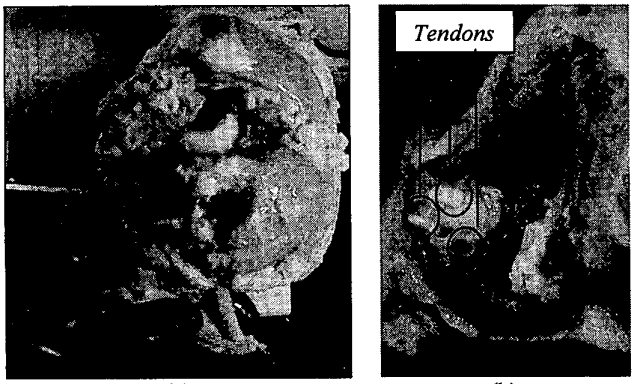

(a) (b)

Figure 4. Chicken tendons around the shoulder joint

As shown in Figure 5, unlike the digital imaging system which is a two-dimensional projection of the external surface, the x-ray imaging system registers a "shadow" cast by a conical x-ray source on the object. The x-ray image properties that are significantly different from the external image are as follows:

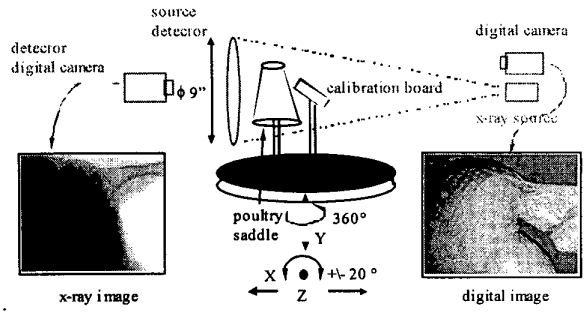

Figure 5. Schematics of the experimental setup

(1) An object with size ϕ_o in length units, and distance, D_{s-o}, from the source casts a "shadow," size ϕ_i, at some distance D_{s-d}. The ratio of the size of the object over the size of its shadow, K, is given by Equation (1). Because of this property, the image seen by the x-ray detector is larger than the actual object.

$$\frac{\phi_o}{\phi_i} = \frac{D_{s-o}}{D_{s-d}} = K \qquad (1)$$

(D_{s-o} = Distance from Source to Object)

(D_{s-d} = Distance from Source to Detector)

(2) The detector camera is located behind the screen so that the image seen by the detector camera is a mirror of the image seen by the digital camera of the external imaging system. The scaled x-ray image is then "flipped."

(3) The nature of an x-ray image is such that it represents all of the 3-D information through the depth of the object in two dimensions. This means that bone structures, which are located behind the area of interest in the viewing angle, will partially or fully occlude the area of interest in the image. Therefore, viewing angles that minimize this occlusion must be used. This tends to limit the angle choices because desired views, such as from the top of the product, are not as clear.

In order to "overlay" the x-ray and the external images so that a correlation between them can be generated, both images are calibrated with respect to a common world frame $(X_w,Y_w,Z_w) = (X_b,Y_b,Z_b)$. Figure 6 shows the coordinate systems of the experimental setup. The coordinate system of the camera (x_c,y_c,z_c) is located at its optical center. The source has its own frame, (x_s,y_s,z_s), as does the detector camera, (X_{dc},Y_{dc},Z_{dc}).

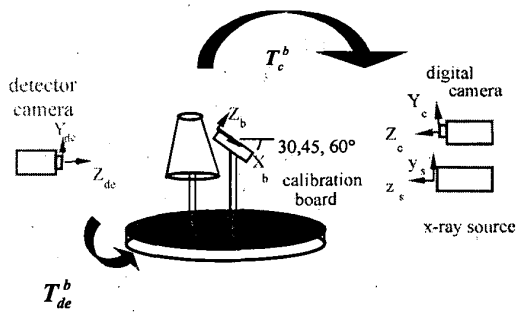

Figure 6. System transformation coordinate frames

The coordinate transformation T_c^b between the camera frame and the world frame and other intrinsic parameters like focal length and lens distortion coefficient are calculated using Tsai Calibration Method [15]. This procedure is repeated for the x-ray image, except that it is "flipped" over and is scaled. The images can then be overlaid using the calibration board origin as the common reference. The results of overlaying the two types of images are summarized in Figure 7. Figures 7(a) and (b) compare the overlay of the two images of the calibration board before and after the correction for the lens distortion and magnification respectively. In Figures 7(a) and (b), the x-ray image is declared as one of the three fundamental colors of the RGB color image, and the edge-detected external feature image is declared in all the RGB layers so that in an overaly it would appear white. It can be seen that in the area of the calibration board most of the circles from both images line up in Figure 7(b). The ovelay of the x-ray and the external images of the bird is shown in Figure 7(c)

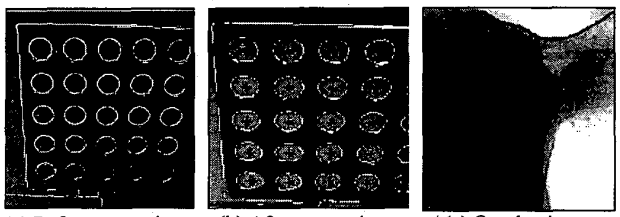

(a) Before correction (b) After correction (c) Overlay image

Figure 7. Overlay of x-ray and external images

To estimate the initial cutting trajectory, a Hough transform can be applied to fit a circle around the bone of interest. The smallest circle, which fully encloses the top of the humerus bone of the product, is a good initial path that automated cutters would follow. Figure 8 illustrates an example result.

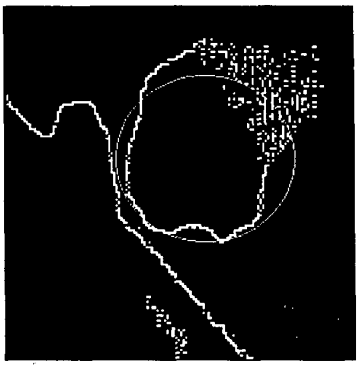

Figure 8. Best-fit initial cutting path

IV. HUMAN 3-D CUTTING TRAJECTORY MODEL

The work described earlier in Section 3 has shown that it is possible to develop a correlation between external surface features and internal structures. Using this knowledge, a model can be developed that locates the joint with respect to surface features, and consequently generates the cutting path. However, the information provided by the 2-D model and cutting path is not sufficient to handle the rather intricate cutting process, which is 3-D in nature. It is possible using multiple views to expand the procedure to obtain 3-D information but thus increases significantly the complexity of the operation. In addition, as we learned more about the cutting process it was realized that we needed knowledge of other internal structures such as tendons and cartilage not easily extracted from x-ray images. To obtain more insight into the cutting procedure, the trajectory and associated forces/torques of the manual cut performed by a human were investigated.

For the deboning task, the desired position and orientation trajectory of the tip is described as a function of time, P(t). The relationship between the tip trajectory and the joint trajectory is in the form:

$$\mathbf{P}(t) = \mathbf{f}(\boldsymbol{\theta}, t) \qquad (2)$$

where $\mathbf{P} \in R^m$ is the position/orientation with respect to the fixed coordinate frame of reference XYZ; and $\boldsymbol{\theta} \in R^n$ is the joint variable vector of the arm and the object manipulating system. For the combined system including the upper extremity and the fixture, n>m and thus the physical system has redundant DOF. The forward solution to Equation (2) is unique for a given joint variable vector. However, the solution to the inverse problem is infinite. We chose to model after a highly skilled cutting expert from the chicken processing plant. For the purpose of designing an automated system, we model the kinetics for the following objectives: The first objective is to determine the joint forces and moments required as a function of cutting force; and the second is to determine the joint trajectory in order to minimize the cutting effort.

A. Experimental Setup

We used a commercially available motion tracking system called Motus©. This system works by tracking retroreflective markers using vision-based technology.

In this experiment, three cameras are used. Another normal video camera is employed to get the digital video of the cutting scene, which will be helpful in identifying markers along with the starting and ending times of the cut. To obtain the movement of the knife, a frame with three non-colinear markers is mounted on the knife (Fig. 5). The three markers are designed such that they have good visibility to all the cameras during the cut, i.e., they are not blocked by other objects and do not overlap with each other. The movement of the three markers is tracked by the Motus system. With known and invariant geometric relationship between the markers and the knife, the six-DOF movement (translation and rotation) of the knife can be obtained.

To acquire the torques/forces during the cutting process, a force/torque sensor is placed between the blade and the handle of the knife. As shown in Figure 9, the sensor measures three forces (x, y, z directions) and three torques (x, y, z directions) in the frame fixed on the sensor. The force/torque signal from the sensor is synchronized with the motion data of the knife.

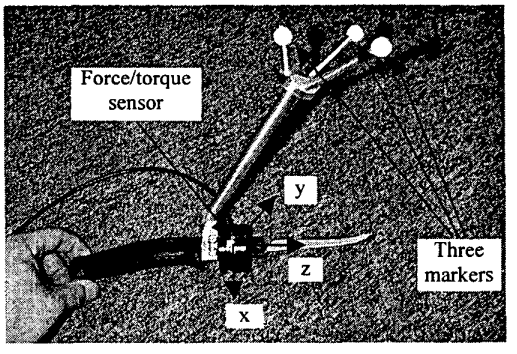

Figure 9. Knife with three markers and F/T sensor

B. Experimental Results

Shown in Figure 10 are the trajectories of the knife tip during several initial wing cuts performed at the left side of what we called the "front-half" of a bird by a deboning expert. Since the original trajectories are rather "noisy" due to the small adjustment motions through the cut, a smooth polynomial interpolation is presented. The trajectories all look similar in that they all curve towards left at the start of the motion to go around the joint and then follow the scapula in a slightly curved motion through the end of the cut.

Figures 11 and 12 show the forces and torques in three directions during the same cut. The observations are summarized as follows:

- During the initial cut, the worker applied a back-and-forth "sawing" motion to the knife to locate the joint and to cut off the tendons around it, which is indicated by the oscillating force along the knife blade (or the z-direction).
- Most of the forces acting on the blade occurred in the direction normal to the knife blade (or in the -x direction), corresponding to large negative torques in the y direction.
- The torque in the direction along the blade (z) is very small compared with torques in other directions, implying that not much twisting around the knife blade was involved in the cut.

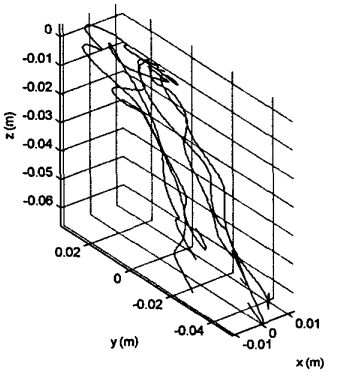

Figure 10. Knife tip trajectory during cut

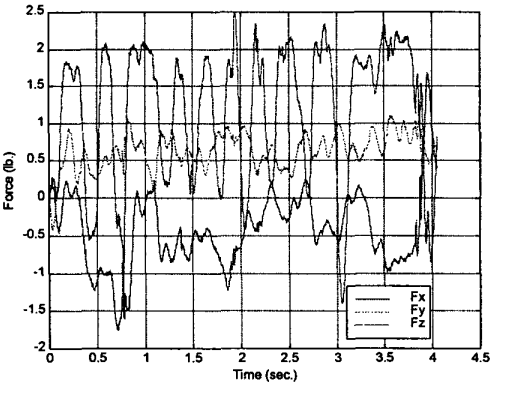

Figure 11. Forces during cut

V. CONCLUSIONS AND FURTHER WORK

A technique has been developed to locate the internal structure (shoulder joint) with respect to the surface features of chicken using x-ray and visual images. Based on the model obtained using this technique, a 2-D cutting path was generated for chicken wing initial cut. Manual cuts performed by a cutting expert have been studied in 3-D space and common

characteristics was found different cuts in terms of the knife motion and the associated cutting forces and torques.

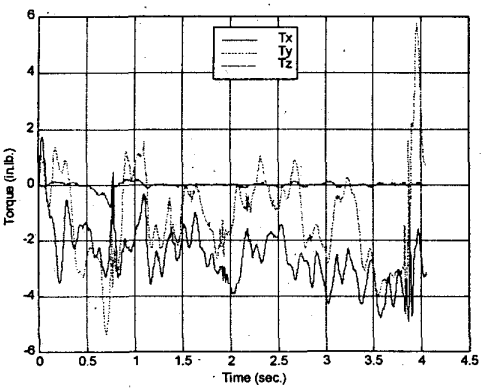

Figure 12. Torques during cut

Further investigations are needed to extract a general cutting path representative of the common characteristics for the cutting procedure from many manual cuts performed by a chicken-processing expert. The cutting path is highly correlated to the deformation and movement of the chicken during the cut, which has to be accommodated in the automated cut. The location where the knife blade is in contact with the chicken moves along the blade during the cut. The simple relationship between the cutting forces and torques is not sufficient to obtain the accurate contact point.

The next phase of the project will be the development of a mechanism utilizing force and torque feedback along with the knowledge of a nominal trajectory correlated to the size and shape of the product to execute the desired trajectory for optimal wing cuts. In the specific system we are working on, a vision system is used to obtain initial cutting point. A multi-DOF robot moves a knife to the initial point and starts the cut. The knife follows the trajectory obtained from expert cutter using the procedure outlined earlier while making adjustments according to force/torque feedback information.

A force/torque feedback mechanism should be developed to adjust the cutting path to accommodate varying sizes and shapes. Force/torque data could be used as threshold between meat (tendon) and bone cutting but the case is much more complicated and a more intelligent strategy needs to be developed.

The knife motion and cutting force/torque data can be used to acquire design specifications in motion range and load capability for an actuator employed in cutting automation.

VI. ACKNOWLEDGMENT

The work described in this paper was done under the auspices of the Office of Food Industry Programs at the Georgia Tech. Research Institute, with funding provided by the State of Georgia through the Georgia Poultry Federation and the Food Processing Advisory Council. We would also like to thank Dr. Robert J. Gregor, Director of the Health & Performance Sciences Department at Georgia Tech., for generously opening up his lab and allowing us use the Motus system. Thanks also go to Dr. Dwight E. Waddell and Ms. Alanna M. Albrecht in the same lab for their support and help with the equipment. We also want to thank Tyson Foods Inc., Cumming, Georgia and the Philips Industrial X-Ray Group, Norcross, Georgia for providing access to their plant and personnel.

VII. REFERENCES

[1] Tuten, Robert (editor), "Watt poultry yearbook, USA edition 1997," p 11, Watt Publishing Company, Morris, IL, 1997

[2] Consumer Reports, "Chicken: what you don't know can hurt you," March 1998, pp. 12-18. Inset: "Working conditions: trouble on the line," pp.16.

[3] Johnson, Member of the Baader Group, Baader 642/650, product information, 1996

[4] FoodCraft, Poultry Modular Breast Deboning System, product information, 1996.

[5] Mycom, Toridas Automated Poultry Leg Deboning Robot, product information, 1995.

[6] Khodabandehloo, K., "Getting down to the bare bones," Industrial Robot, v 16 n 3, Sep 1989, p 160-165.

[7] Purnell, G.; Maddock, N. A.; Khodabandehloo, K., "Robot deboning for beef forequarters," Robotica, v 8 pt 4, Oct-Dec 1990, p 303-310.

[8] Lay, Norbert, "Robotic loin cutting," Proceedings of the Sixth International FAIM Conference (Flexible Automation and Intelligent Manufacturing), p 430-438, May 13-15, 1996, Atlanta, GA.

[9] de Silva, C.W.; Wickramarachchi, N., "An innovative machine for automated cutting of fish," IEEE/ASME Transactions on Mechatronics, v 2 n 2, Jun 1997, p 86-98.

[10] Malone, Denis E.; Friedrich, Werner E.; Spooner, Natalie R.; Lim, Patrick P.K., "Knowledge based control in the processing of highly varying products," Proceedings of the 1994 IEEE International Conference on Robotics and Automation, p 2903-2908, May 08-13, 1994, San Diego, CA.

[11] Jacobs, Jonathan, "Machine vision for meat processing: Making the cut – automatically," Advanced Imaging, v 11, n 11, Nov 1996, 3p.

[12] Harris, S.J.; Mei, Q.; Hibberd, R.D.; Davies, B.L., "Experiences using a special purpose robot for prostate resection," Proceedings of the 1997 8th International Conference on Advanced Robotics, ICAR'97, p 161-166, July 07-09, 1997, Monterey, CA.

[13] Moctezuma, Jose; Bernasch, Jost; Lohmann, Gabriele; Schweikard, Achim; Gosse, Frank, "Robotic surgery and planning for corrective femur osteotomy," Proceedings of the IEEE/RSJ/GI International Conference on Intelligent Robots and Systems. Part 2 (of 3), p 870-877, September 12-16, 1994, Munich, Germany.

[14] Hauser, R.; Westermann, B.; Probst, R., "Non-invasive 3D patient registration for image-guided intranasal surgery - experimental and clinical results," First Joint Conference in Computer Vision, Virtual Reality, and Robotics in Medicine and Medical Robotics and Computer-Assisted Surgery, Grenoble, France, March 1997, pp. 327-336, Springer-Verlag Berlin Heidelberg, Germany, 1997.

[15] Tsai, Roger Y., "A versatile camera calibration technique for high-accuracy 3D machine vision metrology using off-the-shelf TV cameras and lenses," IEEE Journal of Robotics and Automation, v RA3, n 4, p 323-344, Aug 1987.